COMMUNICATION

Mode Converter

ADVANCED
OPTICAL
MATERIALS

www.advopticalmat.d

Check for
updates

Compact Silicon Waveguide Mode Converter Employing Dielectric Metasurface Structure

Hongwei Wang, Yong Zhang, Yu He, Qingming Zhu, Lu Sun, and Yikai Su**

Mode converters are key components in on-chip mode-division multiplexing systems. A compact silicon waveguide mode converter is proposed and demonstrated using all-dielectric metasurface structure with a tilted subwavelength periodic perturbation. The proposed waveguide mode converter can be scaled to realize arbitrary waveguide mode conversion. As examples, two waveguide mode converters are experimentally demonstrated on a silicon-on-insulator wafer, which can convert the TE_0 mode to the TE_1 mode and the TE_2 mode with coupling lengths of 5.75 and 6.736 µm, respectively. The conversion losses of <1 dB and crosstalk values of <−10 dB are achieved for both the TE_0-to-TE_1 and the TE_0-to-TE_2 mode converters.

Advanced multiplexing technologies have been explored to increase data carrying capacity for optical communications and optical information processing.[1–4] On-chip mode-division multiplexing (MDM) technology, which leverages the spatial modes of multimode waveguides,[5–10] allows significant scaling of transmission capacity. Benefitting from its compact footprint and compatibility with the complementary metal-oxide-semiconductor (CMOS) fabrication process, silicon on-chip MDM has attracted much attention. Various MDM devices have been demonstrated on a silicon-on-insulator (SOI) platform, such as mode (de) multiplexers,[9,10] mode converters,[11,12] multimode waveguide bends,[13] and mode-selective switches.[14–17] Among them, mode converters are key components in MDM systems. Many silicon on-chip mode converters have been proposed based on phase matching,[9–11] coherent scattering,[12–14] and beam shaping.[15–17] However, these structures may face the challenges of large footprints, limited operation bandwidth, and relatively large insertion losses. Metasurfaces are 2D artificial materials with subwavelength feature, allowing complete control of the phase, amplitude, and polarization of light beams.[18–24] Integrated optical waveguides with metasurface structures can help address these challenges.

Recently, waveguide mode converters were realized based on gradient metasurface structures consisting of arrays of plasmonic or dielectric nanoantennas.[20] Mode conversions between the trans-electric (TE) modes TE_0, TE_1, and TE_2 were achieved with a length of ≈10 µm at 1550 nm using silicon nanoantennas on $LiNbO_3$ or Si_3N_4 waveguides by simulations.[20] A nanoscale mode converter was theoretically proposed[11] and experimentally demonstrated[21] by introducing a periodic perturbation in its effective refractive index along the propagation direction and a graded effective index profile along its transverse direction. Mode conversion between TE_0 and TE_1 modes was successfully achieved with a length of 23 µm at 1550 nm. However, no experimental results on the crosstalk of the TE mode conversion were provided in the previous reports.[20,21] It is highly desired to miniaturize the device footprint and realize a compact waveguide mode converter.

In this article, we propose and demonstrate a compact silicon waveguide mode converter based on all-dielectric metasurface structure with a tilted subwavelength periodic perturbation. The mode coupling coefficient changes along the propagation direction, which can help the mode conversion process. Our proposed waveguide mode converter can be scaled to realize arbitrary waveguide mode conversion. As examples, we experimentally demonstrate two silicon waveguide mode converters employing all-dielectric metasurface structures that can convert TE_0 mode to TE_1 mode and TE_0 mode to TE_2 mode, respectively. The mode conversion lengths are 5.75 and 6.736 µm for the TE_0-to-TE_1 and TE_0-to-TE_2 waveguide mode converters, respectively, which are shorter than previously reported results.[20,21] Mode demultiplexers are cascaded after the metasurface mode converter to measure the crosstalk values and conversion losses. The insertion losses are lower than 1 dB and the crosstalk values are below −10 dB in a wavelength range of 20 nm for the TE_0-to-TE_1 and TE_0-to-TE_2 waveguide mode conversions.

Figure 1a depicts the 3D view of the proposed waveguide mode converter based on dielectric metasurface structure with a tilted subwavelength periodic perturbation. Propagation of optical field in a perturbed dielectric structure can be described by the coupled mode theory. Attributed to the perturbation on the silicon waveguide, one waveguide mode can be coupled into another mode, and the amplitude of each waveguide mode along the propagation direction is determined by a set of differential equations[11,25]

$$-\frac{\partial A}{\partial z} = j\kappa_{ab}Be^{j(\beta_a - \beta_b)z}$$

$$-\frac{\partial B}{\partial z} = j\kappa_{ba}Ae^{-j(\beta_a - \beta_b)z}$$

(1)

H. Wang, Dr. Y. Zhang, Y. He, Q. Zhu, Dr. L. Sun, Prof. Y. Su
State Key Laboratory of Advanced Optical Communication Systems and Networks
Department of Electronic Engineering
Shanghai Jiao Tong University
Shanghai 200240, China
E-mail: yongzhang@sjtu.edu.cn; yikaisu@sjtu.edu.cn

The ORCID identification number(s) for the author(s) of this article can be found under https://doi.org/10.1002/adom.201801191.
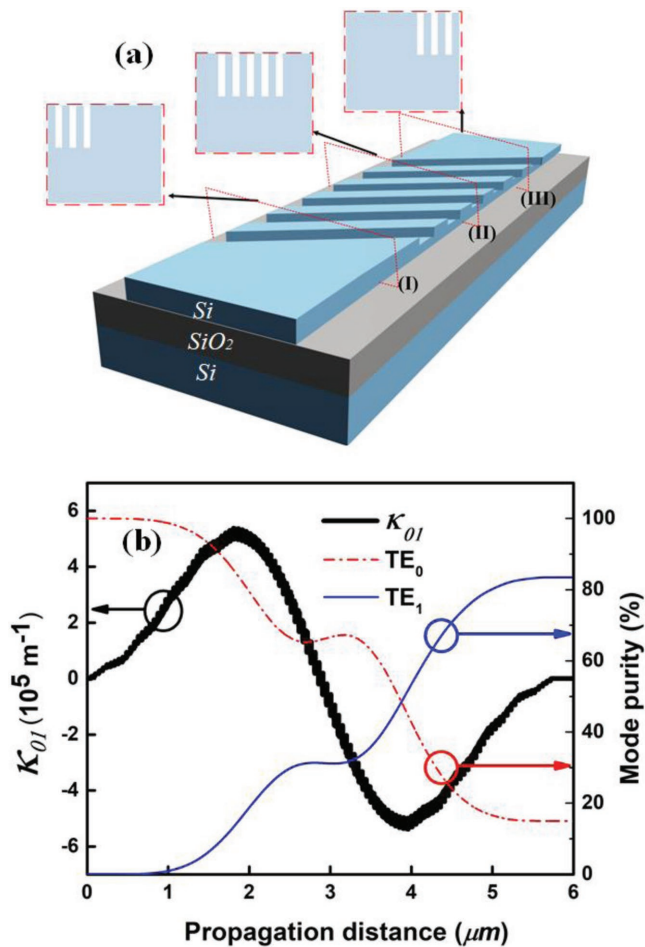
Figure 1. a) Schematic configuration for the proposed waveguide mode converter. Insets show the cross sections at point I, II, and III, respectively. b) Calculated κ_{01} between waveguide modes TE_0 and TE_1 (black thick curve) and the mode purity of TE_0 mode (red dash-dotted curve) and TE_1 mode (blue thin curve) along the propagation direction z. The design parameters of the structure are: period $\Lambda = 400$ nm, period number $n = 5$, the length of the metasurface structure $L = 5.75$ μm, and the width of waveguide $w = 1100$ nm.

where A and B are the amplitudes of waveguide modes a and b, respectively, β_a and β_b are the propagation constants of waveguide modes a and b, κ_{ab} and κ_{ba} represent the exchange coupling coefficients between waveguide modes a and b. The mode coupling coefficient can be defined as[11,25]

$$\kappa_{ab}(z) = \frac{\omega}{4} \iint_S E_a^*(x,y) \cdot \Delta\varepsilon(x,y,z) E_b(x,y)\, dx\, dy \qquad (2)$$

where $E_a(x,y)$ and $E_b(x,y)$ are the electric field profiles of waveguide modes a and b, respectively, S is the cross section of the silicon waveguide, $\Delta\varepsilon(x,y,z)$ is the periodic perturbation in the dielectric waveguide.

Based on Equations (1) and (2), the phase matching condition for the mode coupling between the TE_0 and TE_j mode along the propagation direction z is[11]
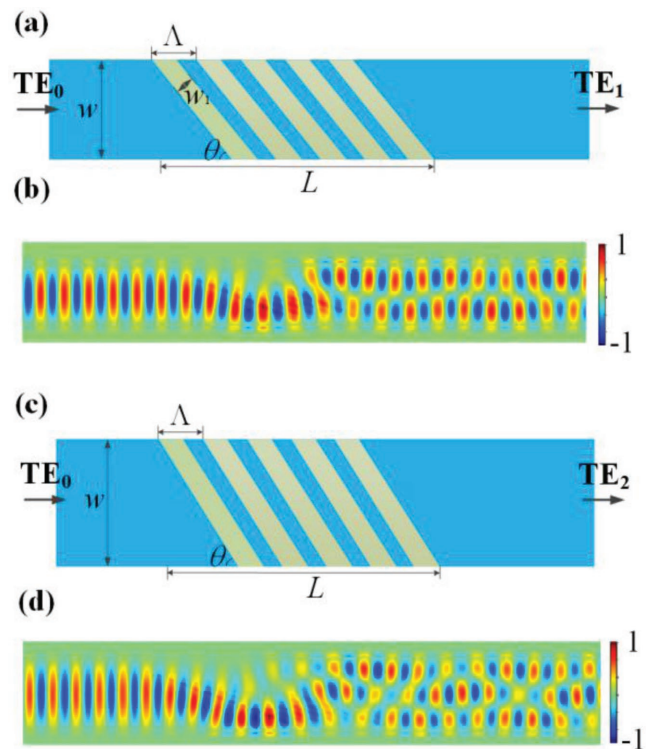
$$\delta = \frac{2\pi}{\beta_a - \beta_b} \qquad (3)$$

Figure 2. a) Top view of schematic configuration and b) simulated E_y distribution for the proposed TE_0-to-TE_1 mode converter. c) Top view of schematic configuration and d) simulated E_y distribution for the proposed TE_0-to-TE_2 mode converter.

where δ is the period of the periodic perturbation $\Delta\varepsilon(x,y,z)$. According to Equation (2), the value of κ_{ab} is related to $\Delta\varepsilon(x,y,z)$, which depends on the cross section of the waveguide. As shown in the insets of Figure 1a, the cross section of the waveguide changes along the propagation direction in the proposed parallelogram metasurface structure. Figure 1b shows the calculated mode coupling coefficient and mode purity of the TE_0 and TE_1 modes along the propagation direction in the TE_0-to-TE_1 mode converter. The TE_0 mode is gradually converted to the TE_1 mode with κ_{01} changing as a sinusoidal-like function along the propagation direction. According to the phase matching condition, the TE_0 mode and the TE_1 mode will be out of phase after propagation over $\delta/2$. Therefore, changing κ_{01} from positive to negative value is required after $\delta/2$ to ensure that the TE_0 mode always contributes constructively to the conversion to the TE_1 mode. Multiple periods of κ_{ab} are needed for mode conversion in the parallelogram metasurface structure. For mode coupling between the TE_0 and TE_j modes, the period number of κ_{0j} should be $(j + 1)/2$, which is related to the field distribution $E_j(x,y)$ of the TE_j mode. So the coupling length is

Table 1. Detailed design parameters for the proposed mode converters.

Mode converter	Width (w) [nm]	Period (Λ) [nm]	Length (L) [μm]	Angle (θ) [degree]
TE_0-to-TE_1	1100	400	5.75	15.5
TE_0-to-TE_2	1400	400	6.736	15.85

**ADVANCED
SCIENCE NEWS**

www.advancedsciencenews.com

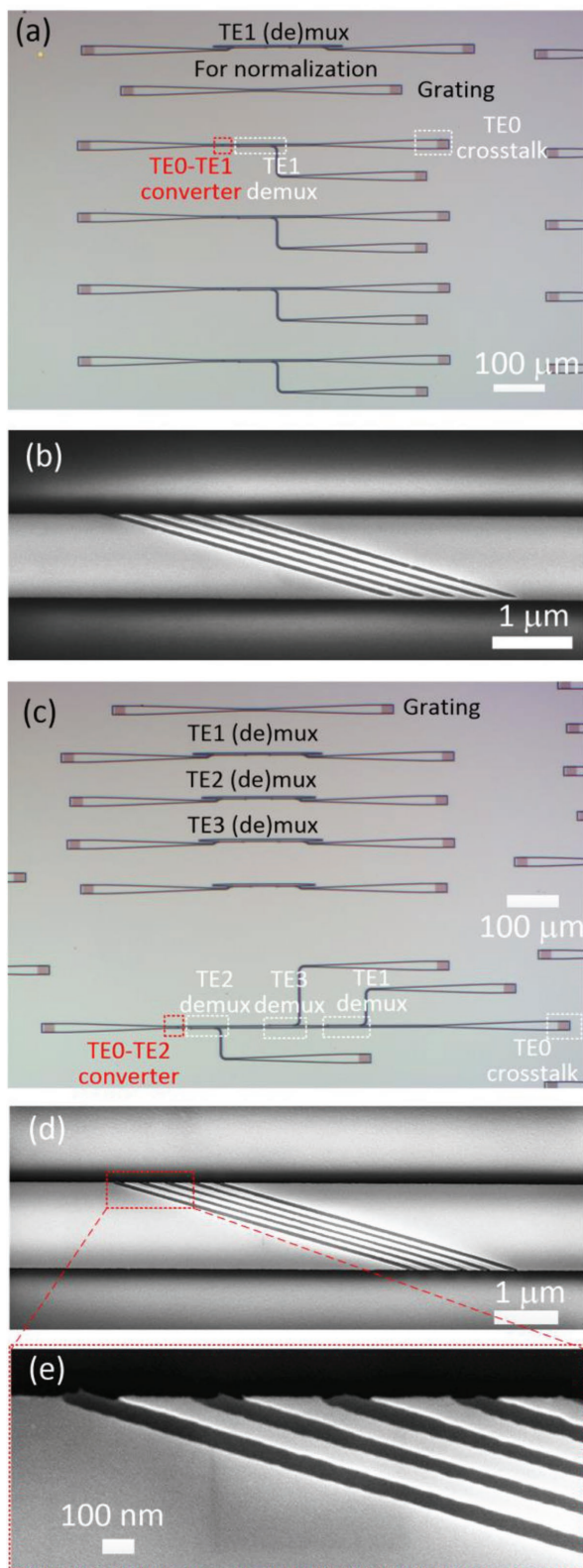**ADVANCED
OPTICAL
MATERIALS**

www.advopticalmat.de

Figure 3. a) Optical microscope photo and b) SEM image of the fabricated TE_0-to-TE_1 mode converter. c) Optical microscope photo and d) SEM image of the fabricated TE_0-to-TE_2 mode converter. e) Magnified SEM image of the metasurface structure.

Table 2. Detailed parameters for the mode (de)multiplexers.

Mode (de)multiplexers	Width of bus waveguide [nm]	Width of access waveguide [nm]	Gap [nm]	Coupling length [µm]
TE_1	1100	540	100	57
TE_2	1400	468	110	40
TE_3	1900	463	100	29

$(j + 1)\delta/2$ and the angle of the parallelogram can be calculated as $\theta = \arctan[2w/((j + 1)\delta)]$. For the TE_0-to-TE_1 and TE_0-to-TE_2 mode converters, the theoretical results of θ are 11.3° and 17.3° with $\delta = 5.535$ µm and $\delta = 3.229$ µm, respectively. The period of the metasurface structure is 400 nm. The feature size (w_1), as shown in **Figure 2**a, is smaller than 50 nm if θ is 11.3°, which is difficult to fabricate in our lab. So θ is selected to be larger than 14.5° in our experiment to relax the fabrication process. Fortunately, the devices show large tolerance to θ variation. Based on such a design specification, we provided design parameters and simulation results of TE_0-to-TE_j ($j = 3, 4$) mode converters in Table S1 and Figure S1 in the Supporting Information, respectively.

Figure 2a shows the top view of the proposed TE_0-to-TE_1 mode converter. Tilted subwavelength periodic perturbations with parallelogram shapes are etched on a silicon waveguide to
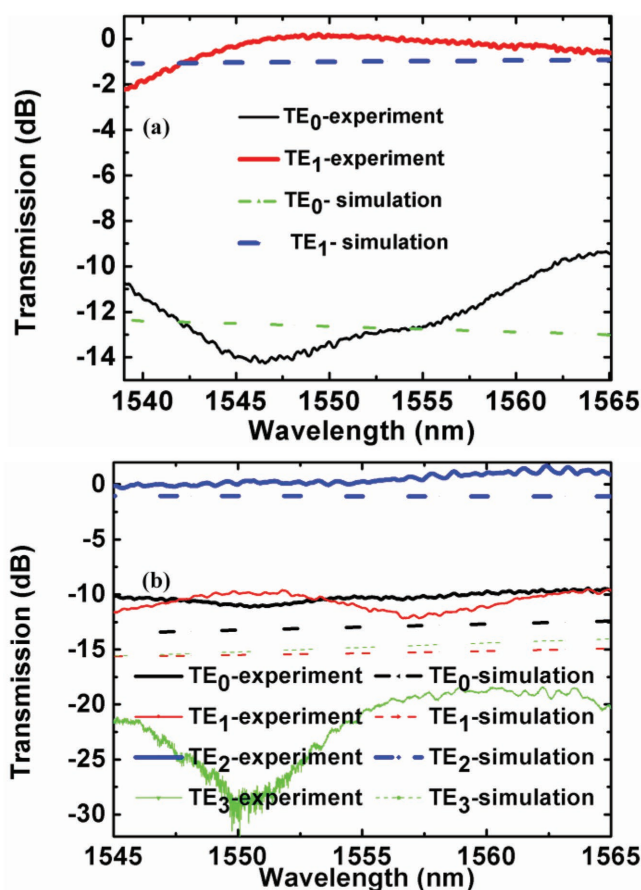

Figure 4. Measured transmission spectra of a) a fabricated TE_0-to-TE_1 mode converter, b) a fabricated TE_0-to-TE_2 mode converter.

**ADVANCED
SCIENCE NEWS**
www.advancedsciencenews.com
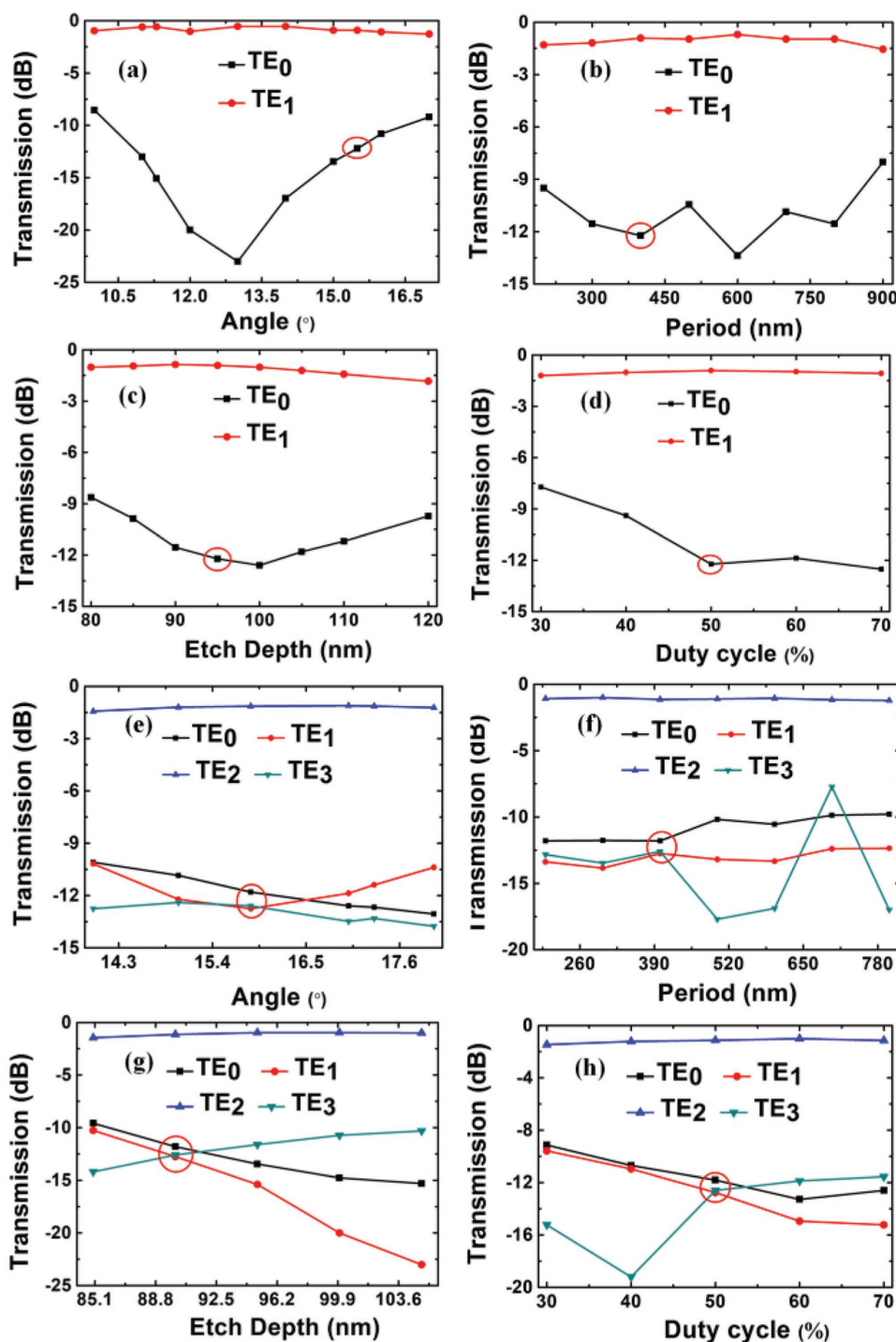
**ADVANCED
OPTICAL
MATERIALS**
www.advopticalmat.de

Figure 5. Simulation results to study the fabrication tolerance. a–d) The transmission loss and crosstalk by changing the angle, period, etch depth, and duty cycle for TE_0-to-TE_1 mode converter. e–h) The transmission loss and crosstalk by changing the angle, period, etch depth, and duty cycle for TE_0-to-TE_2 mode converter. The solid curves represent the simulation results, the red circles represent parameters we used in the experiment.

form dielectric metasurface structures. The width of the silicon waveguide is 1100 nm. The period, duty cycle, etch depth, and angle of the perturbations are 400 nm, 50%, 95 nm, and 15.5°, respectively. The length of the metasurface structure is 5.75 µm. 3D finite-difference time-domain (3D FDTD) method is used to simulate the electric field (E_y) distribution, as shown

in Figure 2b. If the TE_0-mode light is launched into the input port, the light is coupled and converted to the TE_1 mode.

To verify the scalability of our proposed metasurface structure, we also demonstrate a TE_0–TE_2 mode converter. Figure 2c,d shows the top view and simulated E_y distribution of the proposed TE_0-to-TE_2 mode converter. Tilted subwavelength

**ADVANCED
SCIENCE NEWS**

www.advancedsciencenews.com

**ADVANCED
OPTICAL
MATERIALS**

www.advopticalmat.de

Table 3. Comparison of various mode converters.

Structure	Device length [μm]	Device function
Periodically structured waveguide[21]	22.5	TE_0-to-TE_1 (Experiment)
Phase-gradient metasurface[20]	5.4/8.4	TE_0-to-TE_1/TE_2 (Theory)
Microring resonator[7]	25	TE_0-to-TE_1/TE_2 (Experiment)
Directional coupler[27]	30	TE_0-to-TE_1 (Experiment)
Mach–Zehnder interferometer[28]	18	TE_0-to-TE_1 (Experiment)
Compact waveguide taper[29]	20	TE_1/TE_2-to-TE_0 (Theory)
Our work	5.75/6.74	TE_0-to-TE_1/TE_2 (Experiment)

periodic perturbations are etched on a silicon waveguide. The period, duty cycle, etch depth, and angle of the perturbations are 400 nm, 50%, 90 nm, and 15.85°, respectively. The detailed design parameters are provided in **Table 1**. If the TE_0-mode light is injected into the input port, the light is converted to the TE_2 mode over a conversion length of 6.736 μm.

In the experiment, the proposed metasurface mode converters were fabricated on a SOI wafer (220 nm thick silicon on 3000 nm thick silica). Grating couplers, silicon waveguides, and tilted periodic structures were patterned and etched by e-beam lithography (Vistec EBPG 5200+) and inductively coupled plasma etching (SPTS DRIE-I). A tunable continuous wave laser (Keysight 81960A) and an optical power meter (Keysight N7744A) were used to characterize the mode converter devices. The grating couplers were used to couple the light into/out of the chip. The period and duty cycle of the grating coupler are 630 nm and 50%, respectively. The etching depth is 70 nm. The coupling loss was 7.7 dB/port at the central wavelengths of the grating coupler.

Figure 3a,c shows the optical microscope photos of the fabricated TE_0–TE_1 and TE_0–TE_2 mode converters, respectively. To characterize the conversion losses and crosstalk values of the fabricated mode converters, mode (de)multiplexers based on asymmetrical directional couplers[10,26] are cascaded after the mode converters to recover the output higher-order mode signals to TE_0 modes for the measurements. The detailed parameters for the mode (de)multiplexers are shown in **Table 2**. The measured insertion losses of the fabricated mode (de)multiplexers for TE_1, TE_2, TE_3 (de)multiplexing are 4, 9.7, and 8 dB at λ = 1550 nm, respectively. The mode demultiplexers exhibit low intermodal crosstalk and significant mode dependence.[26] The scanning electron microscope (SEM, ZEISS) photos of the fabricated TE_0-to-TE_1 and TE_0-to-TE_2 mode converters are shown in Figure 3b,d,e, respectively.

The measured transmission responses of the fabricated TE_0-to-TE_1 and TE_0-to-TE_2 mode converters are shown in **Figure 4**a and 4b, respectively. The transmission spectra were normalized to that of the identical grating couplers or the mode (de)multiplexers fabricated on the same wafer. For the TE_0-to-TE_1 mode converter, the TE_0-to-TE_1 mode conversion loss is lower than 1 dB and the crosstalk value is below −10 dB in the wavelength range of 1542–1563 nm. For the TE_0-to-TE_2 mode converter, the TE_0-to-TE_2 mode conversion loss is <0.5 dB

and the crosstalk value is <−10 dB in the wavelength range of 1545–1565 nm. The dashed curves in Figure 4 represent the simulated responses of the mode converters using 3D FDTD methods. The discrepancy between the experimental and simulation results may be mainly attributed to the variation of etching depth caused by fabrication errors.

As shown in **Figure 5**, to investigate the fabrication tolerance, we simulated the transmission responses of the devices with different periods, duty cycles, etch depths, and angles by 3D FDTD methods, respectively. For the TE_0-to-TE_1 mode converter, in the range of 11° < θ < 16°, 300 nm < Λ < 800 nm, etch depth varying from 90 to 110 nm and the duty cycle larger than 45%, the insertion losses are <1 dB and the crosstalk values are below −10 dB at λ = 1550 nm. For the TE_0-to-TE_2 mode converter, the insertion losses are less than 1.5 dB and the crosstalk values are below −10 dB at λ = 1550 nm with 15° < θ < 17.6°, Λ < 450 nm, etch depth varying from 90 to 100 nm, and the duty cycle larger than 40%. The simulation results indicate that the devices are tolerant to the variation of period, duty cycle, etch depth, and angle.

Table 3 compares our device with various mode converters with dielectric materials. It indicates that the length of the mode converter is shorter than the previously reported experimental results.

We have proposed and experimentally demonstrated a compact silicon waveguide mode converter implemented with all-dielectric metasurface structure. Attributed to the tilted subwavelength perturbation on the silicon waveguide, the mode coupling coefficient changes along the propagation direction, which can help the mode conversion process. Our proposed waveguide mode converter can be scaled to realize higher-order waveguide mode conversions. Two silicon waveguide mode converters employing all-dielectric metasurface structures are experimentally demonstrated, which can convert TE_0 mode to TE_1 mode and to TE_2 mode, respectively. The mode conversion lengths are 5.75 and 6.736 μm for the TE_0-to-TE_1 and TE_0-to-TE_2 waveguide mode converters, respectively. For the TE_0-to-TE_1 mode converter, the conversion loss is lower than 1 dB, and the crosstalk value is below −10 dB in the wavelength range of 1542–1563 nm. For the TE_0-to-TE_2 mode converter, the conversion loss of <0.5 dB and crosstalk value of <−10 dB are achieved in the wavelength range of 1545–1565 nm. The demonstrated coupling and conversion of waveguide modes provide a general method to manipulate on-chip optical modes, and may find applications in integrated mode-division communication and optical signal processing systems.

Supporting Information

Supporting Information is available from the Wiley Online Library or from the author.

Acknowledgements

Conflict of Interest

The authors declare no conflict of interest.

Keywords

dielectric metasurface, integrated devices, mode converters, silicon

[1] R. Soref, *IEEE J. Sel. Top. Quantum Electron.* **2006**, *12*, 1678.

[2] R. Soref, *Nat. Photonics* **2010**, *4*, 495.

[3] K. Wada, H. C. Luan, D. R. C. Lim, L. C. Kimerling, *Proc. SPIE* **2002**, *4870*, 437.

[4] B. Jalali, S. Fathpour, *J. Lightwave Technol.* **2006**, *24*, 4600.

[5] D. J. Richardson, J. M. Fini, L. E. Nelson, *Nat. Photonics* **2013**, *7*, 354.

[6] P. J. Winzer, *Nat. Photonics* **2014**, *8*, 345.

[7] L. W. Luo, N. Ophir, C. P. Chen, L. H. Gabrielli, C. B. Poitras, K. Bergmen, M. Lipson, *Nat. Commun.* **2014**, *5*, 3069.

[8] B. Stern, X. L. Zhu, C. P. Chen, L. D. Tzuang, J. Cardenas, K. Bergman, M. Lipson, *Optica* **2015**, *2*, 530.

[9] D. X. Dai, J. Wang, S. L. He, *Prog. Electromagn. Res.* **2013**, *143*, 773.

[10] D. X. Dai, J. Wang, Y. C. Shi, *Opt. Lett.* **2013**, *38*, 1422.

[11] D. Ohana, U. Levy, *Opt. Express* **2014**, *22*, 27617.

[12] V. Liu, D. A. B. Miller, S. H. Fan, *Opt. Express* **2012**, *20*, 28388.

[13] Y. Jiao, S. H. Fan, D. A. B. Miller, *Opt. Lett.* **2005**, *30*, 141.

[14] L. H. Frandsen, Y. Elesin, L. F. Frellsen, M. Mitrovic, Y. H. Ding, O. Sigmund, K. Yvind, *Opt. Express* **2014**, *22*, 8525.

[15] H. Guan, Y. J. Ma, R. Z. Shi, A. Novack, J. C. Tao, Q. Fang, A. E. J. Lim, G. Q. Lo, T. Baehr-Jones, M. Hochberg, *Opt. Lett.* **2014**, *39*, 4703.

[16] B. T. Lee, S. Y. Shin, *Opt. Lett.* **2003**, *28*, 1660.

[17] B. B. Oner, M. Turduev, I. H. Giden, H. Kurt, *Opt. Lett.* **2013**, *38*, 220.

[18] X. C. Tong, *Functional Metamaterials and Metadevices*, Springer, Bolingbrook, IL **2018**.

[19] P. Cheben, R. T. Halir, J. H. Schmid, H. A. Atwater, D. R. Smith, *Nature* **2018**, *560*, 565.

[20] Z. Y. Li, M. H. Kim, C. Wang, Z. H. Han, S. Shrestha, A. C. Overvig, M. Lu, A. Stein, A. M. Agarwal, M. Loncar, N. F. Yu, *Nat. Nanotechnol.* **2017**, *12*, 675.

[21] D. Ohana, B. Desiatov, N. Mazurski, U. Levy, *Nano Lett.* **2016**, *16*, 7956.

[22] A. Y. Piggott, J. Lu, K. G. Lagoudakis, J. Petykiewicz, T. M. Babinec, J. Vučković, *Nat. Photonics* **2015**, *9*, 374.

[23] S. Jahani, Z. Jacob, *Nat. Nanotechnol.* **2016**, *11*, 23.

[24] D. Lin, P. Fan, E. Hasman, M. L. Brongersma, *Science* **2014**, *345*, 298.

[25] A. Yariv, P. Yeh, *Optical Waves in Crystals: Propagation and Control of Laser Radiation*, Wiley, Hoboken, NJ **2002**.

[26] C. C. Gui, Z. L. Zhang, D. S. Gao, C. Li, Q. Yang, presented at CLEO, San Jose, CA, June **2014**.

[27] Y. H. Ding, J. Xu, F. D. Ros, B. Huang, H. Y. Ou, C. Peucheret, *Opt. Express* **2013**, *21*, 10376.

[28] Y. Y. Huang, G. Y. Xu, S. T. Ho, *IEEE Photonics Technol. Lett.* **2006**, *18*, 2281.

[29] D. G. Chen, X. Xiao, L. Wang, Y. Yu, W. Liu, Q. Yang, *Opt. Express* **2015**, *23*, 11152.